Epithelium-dependent Extracellular Matrix Synthesis in Transforming Growth Factor-β1–Growth-inhibited Mouse Mammary Gland

Gary B. Silberstein, Phyllis Strickland, Susanne Coleman, and Charles W. Daniel

Department of Biology, Sinsheimer Laboratories, University of California, Santa Cruz, Santa Cruz, California 95064

Abstract. Exogenous transforming growth factor beta (TGF-β1) was shown in earlier studies to reversibly inhibit mouse mammary ductal growth. Using small plastic implants to treat regions of developing mammary glands in situ, we now report that TGF-β1 growth inhibition is associated with an ectopic accumulation of type I collagen messenger RNA and protein, as well as the glycosaminoglycan, chondroitin sulfate. Both macromolecules are normal components of the ductal extracellular matrix, which, under the influence of exogenous TGF-β1, became unusually concentrated immediately adjacent to the epithelial cells at the tip of the ductal growth points, the end buds. Stimulation of extracellular matrix was confined to aggregations of connective tissue cells around affected end buds and was not present around the TGF-β1 implants themselves, indicating that the matrix effect was epithelium dependent. Ectopic matrix synthesis was specific for TGF-β1 insofar as it was absent at ducts treated with other growth inhibitors, or at ducts undergoing normal involution in response to endogenous regulatory processes. These findings are consistent with the matrix-stimulating properties of TGF-β1 reported for other systems, but differ in their strict dependence upon epithelium. A possible role for endogenous TGF-β1 in modulating a mammary epithelium–stroma interaction is suggested.

TRANSFORMING growth factor beta-1 (TGF-β1)[1] and its receptors are ubiquitous in cells from both developing and mature tissue, and the factor is capable of modulating the growth and differentiation of a wide variety of cell types (1, 16). TGF-β1 also stimulates the synthesis and deposition of extracellular matrix both in vivo and in vitro, as well as hastening wound healing by promoting the synthesis of fibrous connective tissue (15). A developmental role for TGF-β1 is implied by its localization in a variety of organs, and by the finding that mesoderm induction by fibroblast growth factor in *Xenopus* embryos probably requires a TGF-β-like factor (11). In addition, Mullerian inhibiting substance (MIS), a peptide factor related to TGF-β1, causes the programmed resorption of the female urogenital anlagen in fetal males (23).

The mouse mammary ductal system grows by repeated, dichotomous branching that results in a highly arborated ductal tree connected at its base to the nipple (Fig. 1 a). Although most of this growth occurs postpartum it is, by several criteria, similar to the embryonic morphogenesis of branched organs such as the salivary gland, kidney, and lung, particularly with respect to the localization and dynamics of extracellular matrix, which develops adjacent to growth-points (in the mammary gland, the end buds) (2). In each case the matrix comprises collagens, glycosaminoglycans, fibronectin, laminin, and proteoglycans (19, 24). Both in vitro and in vivo studies have shown that growth and differentiation of mammary ductal cells are dependent on the extracellular matrix (3, 18).

The branching growth of mammary ducts, as well as growth inhibition, involve a complex interplay of epithelium and mesenchyme that is characterized by the ongoing, highly localized replacement of fatty stroma by fibrous extracellular matrix at the interface of the two tissues (Fig. 1 c) (19, 20, 24). This fibrous condensate forms along the end bud flanks and surrounds the narrowing duct, giving rise to a collagenous sheath that invests the entire ductal tree, with the exception of the end bud tips, which, during active growth, are invariably free of fibrous investment. This organization of fibrous connective tissue is an example of a developmental tissue interaction, as it is clear that the epithelium induces the formation of its stroma-derived fibrous tunic. As with other examples of epithelium–mesenchyme interaction in branching morphogenesis, the molecular signals responsible for regulating the localization, synthesis and deposition of ductal extracellular matrix are unknown.

In other studies (7, 21) we showed that localized TGF-β1 treatment inhibited mouse mammary ductal growth in situ. Terminal ducts from glands treated for 4 d resembled un-

---

1. *Abbreviations used in this paper:* ECM, extracellular matrix; MIS, Mullerian inhibiting substance; S-GAG, sulfated glycosaminoglycans; TGF-β1, transforming growth factor-beta 1.

treated terminal ducts in which growth was inhibited by normal regulatory process, suggesting that TGF-β1 may be a natural growth regulator in the gland (21). This suggestion is supported by the observation that whereas TGF-β1 rapidly and selectively inhibited ductal DNA synthesis, lobuloalveolar DNA synthesis was unaffected (7). The capacity of TGF-β1 to modulate the synthesis and deposition of extracellular matrix components in a variety of nonmammary systems, and the importance of the matrix in normal ductal growth, suggested that exogenous TGF-β1 might affect the ductal extracellular matrix. Using plastic implants to treat mammary ducts in situ, we now report that short-term (12–24 h) treatment with TGF-β1 stimulated extensive extracellular matrix deposition that was localized at the end bud tip, a zone normally free of fibrosis during active growth, suggesting a role for TGF-β1 as a modulator of epithelium–stroma interactions.

Materials and Methods

Animals and Implants

C57 females at 5 wk of age showing extensive end bud growth were used for these implant studies. Procedures for EVAc implant preparation and surgical implantation as well as alcian blue staining are described in detail elsewhere (21, 22).

Tissue Techniques

For general histology glands were fixed for 12 h in either Tellyesniczky's or Carnoy's fixative. For whole mount preparations, glands were defatted for 3 h in three changes of acetone, stained 3 h with hematoxylin (0.65 g FeCl₃; 67.5 ml water; 8.7 ml 10% hematoxylin in 95% ethanol; 1000 ml 95% ethanol, pH adjusted to 1.25 with concentrated HCl), dehydrated through graded alcohols to xylene, and photographed. After whole-mount examination, pieces of tissue were embedded in paraffin and 5-μm sections were deparaffinized, rehydrated, and stained with alcian blue. The cationic dye, alcian blue, stains glycosaminoglycans and was used to demonstrate glycosaminoglycan-rich extracellular matrix as well as to delineate the epithelial–stromal boundary. For simultaneous staining of both hyaluronate and sulfated glycosaminoglycans, the dye solution contained 0.1% dye in 0.025 M sodium acetate, pH 5.8, with 0.3 M MgCl₂ (7). Staining time was 45 min. The prior hematoxylin stain did not affect this secondary staining.

Sirius red F3BA (Mobay, Inc., Pittsburgh, PA), is an azo dye with high specificity for collagen. Tissue sections fixed as above were stained for 30 min in a mixture of 0.1% Sirius red and 0.1% Fast Green, a counterstain, dissolved in saturated picric acid (12). Digestion of sections with collagenase before staining eliminated Sirius red–stained material in the tissue (not shown).

Three-dimensional Reconstructions

Using a drawing attachment, the outlines of end buds and adjacent fibrous stroma were traced directly from microscope images of serial sections of treated and control end buds. Traced images were digitized using a digitizing pad (Summagraphics), and reconstructed using three-dimensional reconstruction software developed by The Laboratory for High Voltage Electron Microscopy, University of Colorado.

Sulfated Glycosaminoglycan Synthesis

Autoradiographic localization of sulfated glycosaminoglycans has been described by us in detail (19). Briefly, carrier-free H₂SO₄ is injected intraperitoneally and 3 h later the animal is killed. Tissue is then fixed and sectioned and autoradiography is carried out using standard methods. Chondroitinase ABC (Sigma Chemical Co., St. Louis, MO) (2.5 U/ml in 0.1 M Tris HCl, pH 8.0, 37°C for 4 h) was used on sectioned material to determine the extent of sulfur incorporation into chondroitin sulfate.

In Situ Hybridization

Probe. A 1.3-kb fragment containing the coding region for rat alpha 1 (I) collagen (isolated by Dr. David Rowe, University of Connecticut) was cloned by Dr. Steven Feitelberg (University of California, San Diego) into an SP6/T7 plasmid (pGEM, Promega Biotec, Madison, WI). High specific activity sense (control) and antisense RNA probes using [³⁵S]UTP (1,200 Ci/mmol) were made using Promega Biotec transcription reaction protocol no. 1. Probes were sized by limited alkaline hydrolysis to ~150 bp.

Tissue. A modification of the Cox et al. hybridization protocol was followed (6). Briefly, tissue was fixed in 4% paraformaldehyde for 3 h, dehydrated through graded alcohols to xylene and paraffin embedded; 10-μm sections were deparaffinized and pretreated with 1.0% BSA, followed by 0.2 N HCl, then digested with 1 μg/ml proteinase K (in 20 mM Tris, 2 mM CaCl, pH 7.5), to improve probe access. Sections were then postfixed in 4% paraformaldehyde, blocked with 0.2% glycine and treated with 0.25% acetic anhydride in 0.1 M triethanolamine to acetylate positive charges on the slide or tissue.

Blocking Probes. Using a variety of antisense probes, including that for type I collagen, we observed heavy, nonspecific hybridization in the condensed stroma around treated and control end buds. This problem was overcome by adding a blocking hybridization step utilizing "irrelevant," cold mRNA transcripts. For convenience, we used the three transcripts generated by T7 polymerase from the Promega phage lambda "control templates" (1.38, 0.55, and 0.22 kb, respectively). Each slide was incubated with 4 μg of lambda mRNA in hybridization buffer (see below) for 16 h at 56°C. After incubation, slides were washed in four changes of 2× SSC for 1 h and air dried before proceeding.

Hybridization. To each slide, 1 × 10⁶ cpm were added in 40 μl hybridization buffer (50% formamide, 300 mM NaCl, 10 mM Tris, 1 mM EDTA, 1× Denhardt's, 10% PEG, 100 mM DTT, 25 U RNasin [Promega Biotec] and 150 μg/ml tRNA); incubation was overnight at 56°C with coverslips sealed with rubber cement to prevent changes in hybridization volume. All posthybridization washes contained DTT. Slides were washed in 2× SSC containing 50 mM DTT, treated with 20 μg/ml RNase A (Calbiochem-Behring Corp., La Jolla, CA), 30 min, 37°C, (without DTT), washed in RNase buffer (with 5 mM DTT), 5 liters 2× SSC (with 1 mM DTT), 50% formamide in 2× SSC, 1% SDS (with 1 mM DTT) at 50°C for 1 h and at 65°C for 5 min and a final wash of 2× SSC for 5 min. Slides were air-dried and dipped in NTB-2 emulsion diluted 1:1 with water. Slides were exposed for 2 d and developed in D-19 developer.

Control Tissue. On each slide there were sections of 5-wk mammary gland that had been implanted for 24 h with 120 ng TGF-β1 as well as sections of control gland treated with nonreactive BSA. Longitudinal sections of (15-d) mouse embryo were included on each slide and showed specific localization of collagen 1 message in chondrocytes and skin (not shown).

Results

In mammary gland branching morphogenesis, the tips of rapidly growing ducts are enlarged, forming highly mitotic, bulbous end buds (Fig. 1, *a* and *c*). A basal epithelial monolayer consisting of myoepithelial stem cells, the cap cells, overlays the body of the end bud; during ductal growth these cells are normally apposed to adipocytes (Fig. 1 *c*). In response to exogenous TGF-β1, end buds are rapidly replaced by nonproliferating ductal tips (Fig. 1 *b*). Earlier studies had shown that after 4 d, TGF-β1-treated ducts were morphologically similar to ducts from untreated, growth-quiescent glands with respect to epithelial histo-architecture particularly the differentiation of the cap cells. The organization of adjacent fibrous connective tissue at 4 d was also similar in treated and control tissue (21).

Early Effects of TGF-β1 Treatment on Collagen Gene Expression

Recent in vitro experiments have shown that TGF-β1 stimulation of collagen and fibronectin mRNA synthesis in mouse 3T3 cells occurs within a narrow time-frame of 12–24 h after
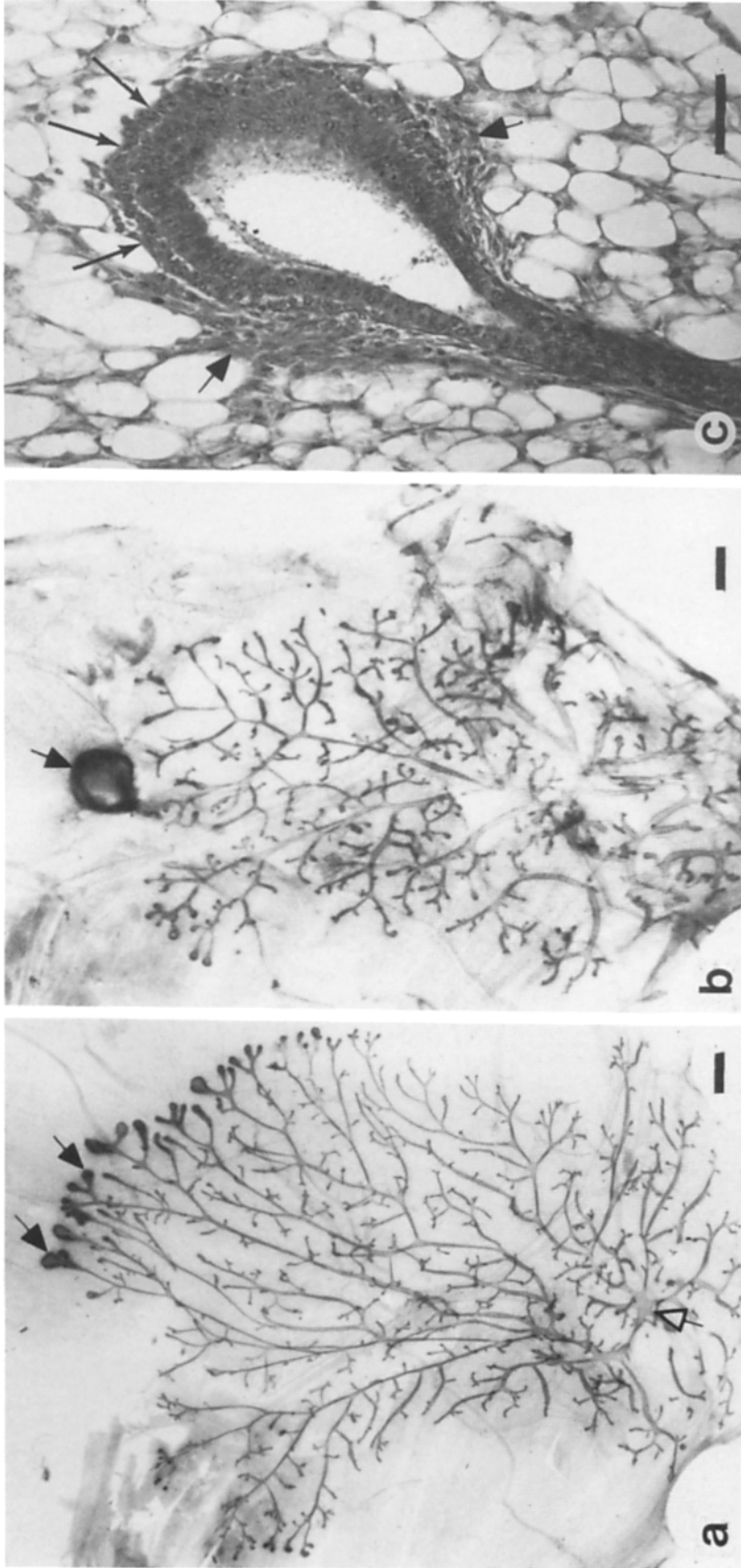
Figure 1. Photomicrographs of normal mammary gland from 5-wk-old animal. (*a*) Whole-mount preparation. End buds (*solid arrows*) are visible at the tips of ducts at the top of the gland. Nipple is at the base of the gland (*open arrow*). (*b*) TGF-β1 implant (*arrow*, 500 ng), in place for 4 d, caused involution of end buds. (*c*) Untreated end bud. The cap cell layer is visible (*small arrows*) adjacent to adipocytes. A fibrous sheath begins along the flank (*large arrows*) and extends to the rear, investing the mature ducts. Bar, 50 μm. (Reproduced from *Science [Wash. DC]*., 1987, 237:291–293, by copyright permission of the American Association for the Advancement of Science) (21).
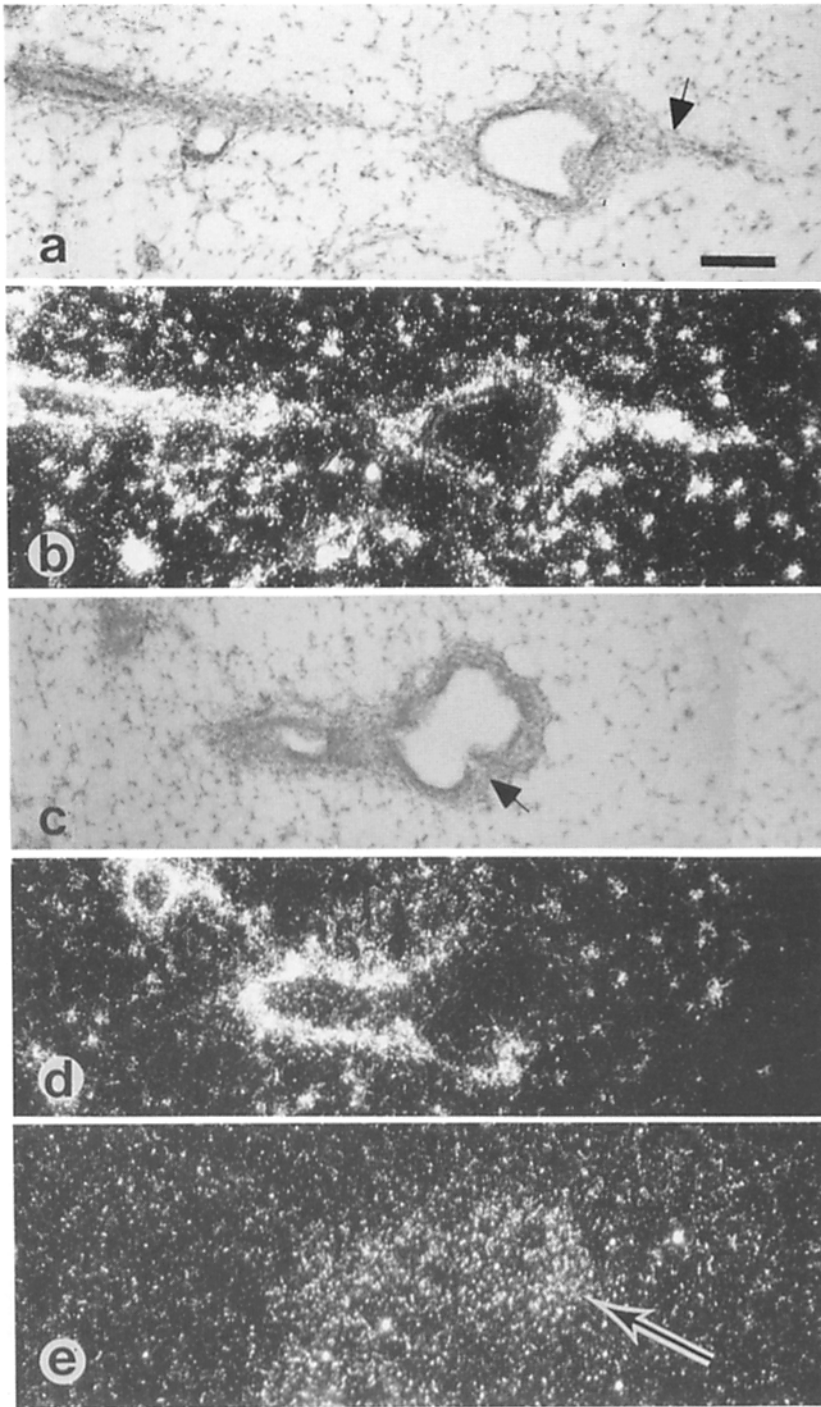
Figure 2. Localization of type I collagen message by in situ hybridization. (*a* and *b*) Light- and dark-field micrographs of an end bud in the vicinity of a TGF-β1 implant (150 ng) for 24 h. Cellular connective tissue (*arrow*) and heavy hybridization are apparent over the tip of the end bud. (*c* and *d*) Light- and dark-field micrographs of an untreated end bud. There is no labeling over the tip except where a cleft is forming (*arrow*). Both treatment and control tissues showed similar levels of labeling over the flanks and subtending duct. (*e*) Tissue exposed to sense mRNA probe. End bud (*arrow*) had slightly higher than background labeling but no specific localization was observed. Bar, 50 μm.

treatment (13), suggesting the importance of investigating effects of TGF-β1 occurring before the 4-d time period of our earlier report (21). To carry out this study we treated ducts in 5-wk, virgin animals for 24–48 h with doses of TGF-β1 known to inhibit growth, and examined effects on the extracellular matrix.

Type I collagen, a dominant component of fibrous matrix, is normally associated with the periductal matrix but does not occur in quantity around the tips of growing end buds (19, 24). Using antisense mRNA from the rat alpha 1(I) collagen gene for in situ hybridization, we examined collagen gene ex-

pression around untreated end buds and those treated for 24 h in situ with TGF-β1. In treated glands, heavy labeling was usually found in stroma adjacent to the cap cell layer at the growing tip (Fig. 2 *b*), and was typically organized into one or more conspicuous strands extending ahead of the end bud tip into the stroma. Histologically, the collagen message colocalized with a conspicuous structure consisting of fibrocytes and alcianophilic matrix (Fig. 2 *a*).

In untreated glands there was heavy collagen I gene expression on the end bud flank and subtending duct, whereas only background levels were observed at the end bud tips
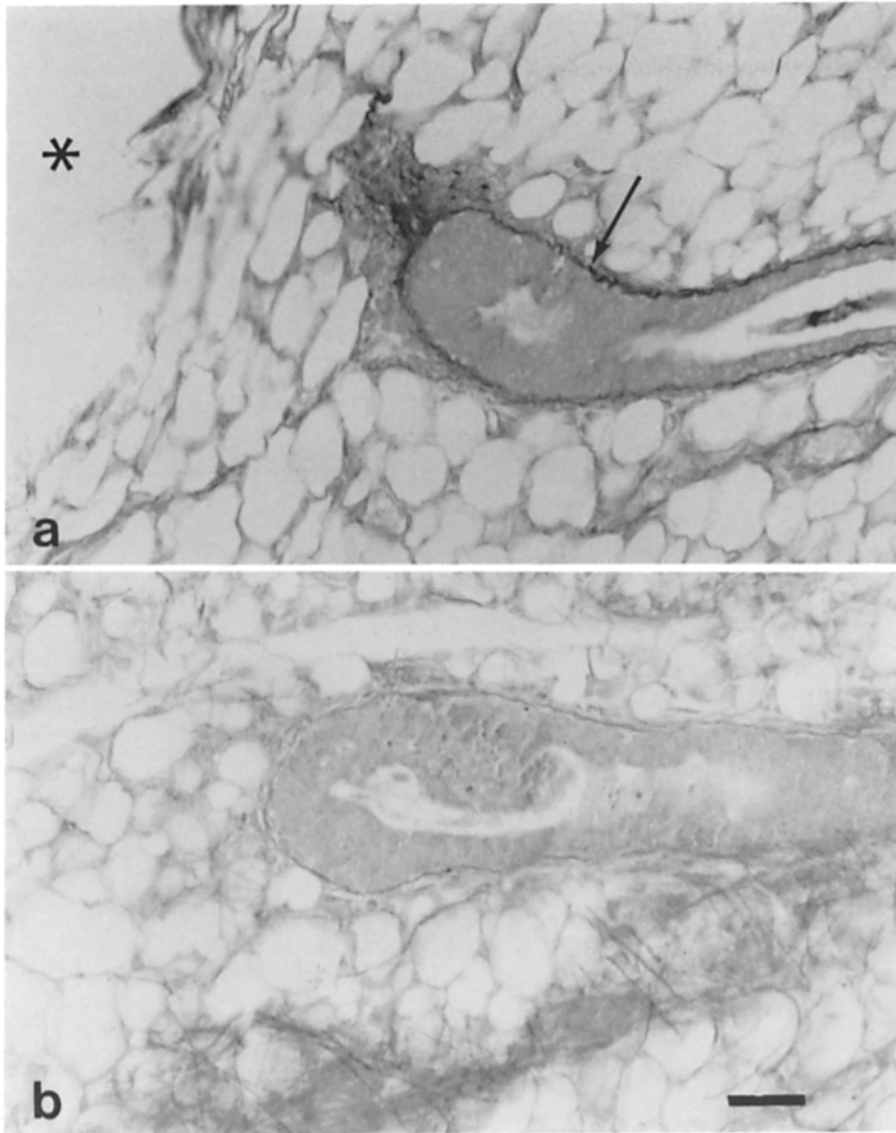
Figure 3. Photomicrographs illustrating the effects of TGF-β1 (150 ng/15 h) on collagen distribution around an end bud and adjacent implant (*a*); control duct (*b*). Bar, 50 μm. Tissue sections were stained with the collagen-specific dye, Sirius red (see Materials and Methods). The periductal collagenous sheath appeared to stain more heavily in the TGF-β1-treated duct (*arrow*), less so in the control. In the treated gland, some stain was visible within the dense, cellular mass adjacent to the end bud tip. Note the absence of stain or dense cellularity around the TGF-β1 implant (*). The heavily stained fibers beneath the control duct are part of collagenous septae, a normal feature of the gland.

(Fig. 2, *c* and *d*). Treated tissue showed the same pattern of labeling in the flank and subtending duct as the control (Fig. 2, *b* and *d*), indicating that treatment did not influence the expected high level of periductal collagen gene transcription.

To determine if gene expression was accompanied by deposition of collagen fibers, TGF-β1-treated tissue was stained with the collagen-specific dye, Sirius red (Fig. 3 *a*). A few fibers of deeply stained collagen were visible in the dense cellular mass over the end bud tip, but most of the matrix stained lightly and appeared amorphous. The absence of conspicuous stain around the TGF-β1 implant and between the duct tip and the implant was noted. Untreated gland, in which end buds were involuting due to normal regulatory processes, showed only a thin layer of Sirius red staining at the tip (Fig. 3 *b*).

Tissue sections passing through the plastic implants were examined and no organized areas of increased collagen gene activity were observed around either the TGF-β1 or the control implants (Fig. 4). Scattered foci of collagen mRNA synthesis were found throughout the stroma, in a punctate

pattern similar to that described for the skin (17). Thus, organized areas of intense mRNA synthesis occurred only in stroma at the end bud tip in TGF-β1-treated gland, and in a periductal location in all glands, and therefore appeared to be unrelated to placement of the TGF-β1 implant. As expected, no labeling above background was found over any mammary epithelial tissues.

TGF-β1 Effects on Synthesis of Sulfated Glycosaminoglycans

Sulfated glycosaminoglycans (S-GAG) are constituents of matrix proteoglycans, and are a major component of the periductal matrix (19, 20). TGF-β1 has been shown to induce chondroitin sulfate synthesis in mammary cells in vitro (14). Staining with the cationic dye alcian blue indicated heavy accumulations of S-GAG at the tip of TGF-β1-treated end buds (Fig. 5 *a*) (19, 20). To investigate the biosynthesis of S-GAG, radiolabeled sulfur incorporation was studied. The stroma around TGF-β1 affected end buds showed extensive ^{35}S in-
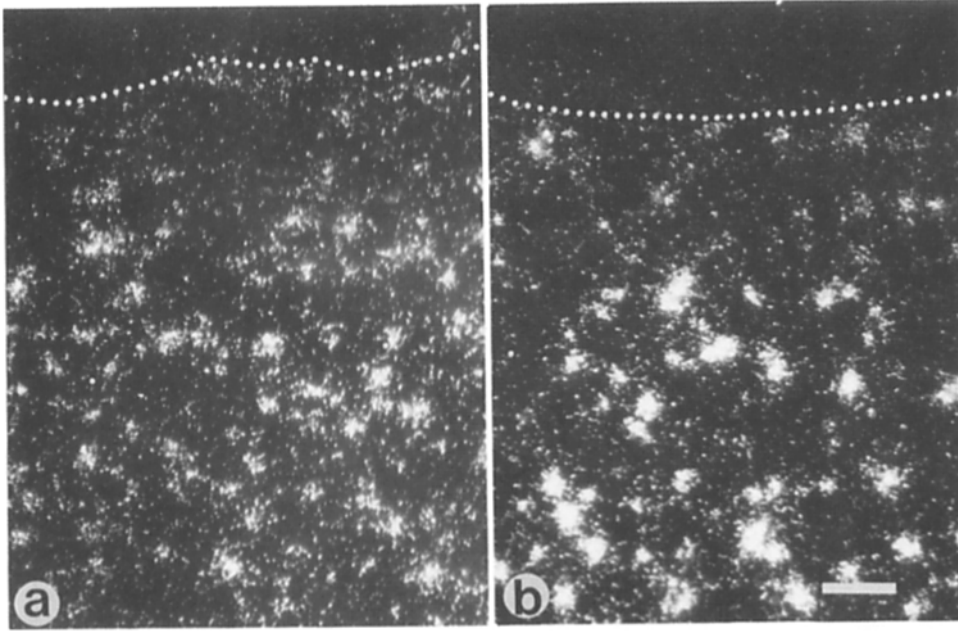
Figure 4. In situ localization of type I collagen message in tissue adjacent to (*a*) BSA-containing or (*b*) TGF-β1-containing implant (dotted line marked implant boundary). TGF-β1 did not induce a message-containing capsule around the implant. Scattered foci of hybridization appear in the adipose tissues in approximately equal numbers in treatment and control. The density of the focal signals appeared greater in the TGF-β1-treated gland pictured here, though this was not consistently observed. Bar, 50 μm.

corporation, extending well beyond the end bud tip. In sections of TGF-β1-treated end buds digested with chondroitinase ABC, a significant amount of label was removed (Fig. 6), indicating that much of the incorporated sulfur was contained in chondroitin sulfates. The heavy incorporation of ^{35}S in the stroma, the low level of labeling over the epithelium, and the relatively short labeling time, suggest that the bulk of the labeled molecules were synthesized directly in the stroma and not transported from the epithelium.

In contrast to the TGF-β1-affected tissues, control end buds showed only light alcian blue staining above the cap zone, with characteristically heavy staining on the flanks and subtending ducts (Fig. 5 *c*); ^{35}S was concentrated in the latter zone and was only lightly deposited on the caps (Fig. 5 *d*).

TGF-β1 enhancement of S-GAG synthesis was also found to be mediated by mammary epithelium. Examination of TGF-β1 implants showed no accumulation of alcianophilic material in surrounding stroma, and there was no stimulation of sulfur incorporation on the border of the TGF-β1 implants (Figs. 5 and 6).

Effect of Growth Inhibition on Ductal ECM

The observation of intense ECM synthesis at TBF-β1-inhibited end bud tips left open the question of specificity of action. We were interested in determining if the effect was specific to exogenous TGF-β1 or, alternatively, if growth inhibition and matrix synthesis may be tightly coupled and, whether achieved by TGF-β1 or another growth inhibitor, inevitably results in heavy matrix deposition over the end bud tip.

Comparing normally involuted and TGF-β1-treated ducts, heavy matrix concentrations were never seen at the ductal tips in untreated glands (Figs. 7, *a* and *b* and reference 19). Three dimensional reconstructions of matrix disposition demonstrated that even in the early stages of involution, where the end bud shape is still evident, the extracellular matrix merely envelopes the tip of the untreated end bud rather than extending far beyond it (Fig. 7, *d* and *e*).

To investigate the possibility that inhibition of epithelial DNA synthesis by other exogenous agents could result in heavy matrix accumulation over the end bud tip, inhibitors other than TGF-β1 were tested. Implantation of EGF produced localized inhibition of end bud growth (5), but in no case were heavy ectopic matrix accumulations observed (Fig. 7 *c*). Implanted dexamethasone, another reversible inhibitor of ductal growth, also did not lead to unusual matrix accumulation (not shown).

Discussion

Matrix-inducing properties of TGF-β1 are now well described and are characterized by the rapid and coordinated synthesis of many matrix elements, including type I collagen and chondroitin sulfate, by cultured cells, as well as by the inhibition of synthesis of matrix-degrading enzymes (15). In this paper we show that within 24–48 h, growth inhibition by implanted TGF-β1 was associated with highly localized, intense collagen I gene expression and synthesis of sulfated glycosaminoglycans (Figs. 2, 3, 5, and 6). This stromal response occurred in an unusual location, ahead of the end bud, and thus differed from the progressive investment of the tip by extracellular matrix extending up the sides of the end bud that occurs in normal involution or in response to growth inhibitors such as EGF or dexamethasone (Fig. 7) (5, 20).

The use of plastic implants to administer TGF-β1 in situ permitted us to distinguish between matrix formation that was a response to epithelium–stroma interactions, and generalized induction of stromal matrix elements. Short-term treatment with TGF-β1 did not result in intense matrix synthesis at the site of the implant; instead, matrix often formed up to a millimeter away from the implant and was confined to a zone at the tip of the end bud epithelium.
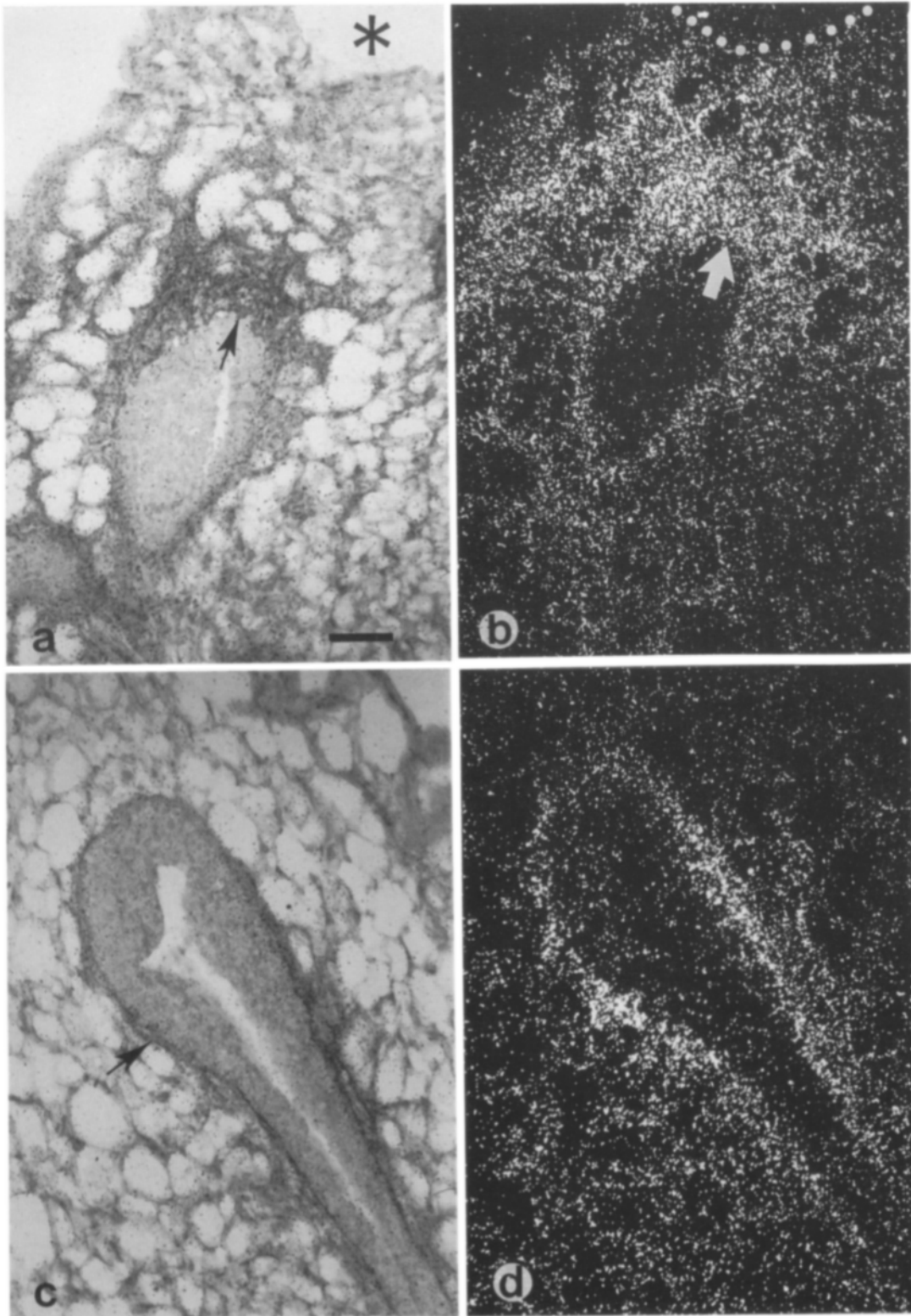
The action of TGF-β1 on matrix synthesis clearly required

Figure 5. Photomicrographs of alcian blue stained, ^{35}S autoradiographs showing incorporation of radiolabeled sulfur into TGF-β1 treated (150 ng/24 h) and untreated tissue. Light (*a* and *c*) and dark-field (*b* and *d*) micrographs are shown. (*a* and *b*) TGF β1-treated gland. Note the heavy concentration of label around the tip of the end bud. (Arrow indicates epithelial–stromal interface.) Implant is at upper right and is indicated by asterisk in *a* and a boundary of white dots in *b*. (*c* and *d*) Control. Note the heavy concentration of label on the end bud flank (*arrow*) and subtending duct and the lighter labeling on the tip. In all cases, labeling colocalized with alcianophilia. Bar, 50 μm.
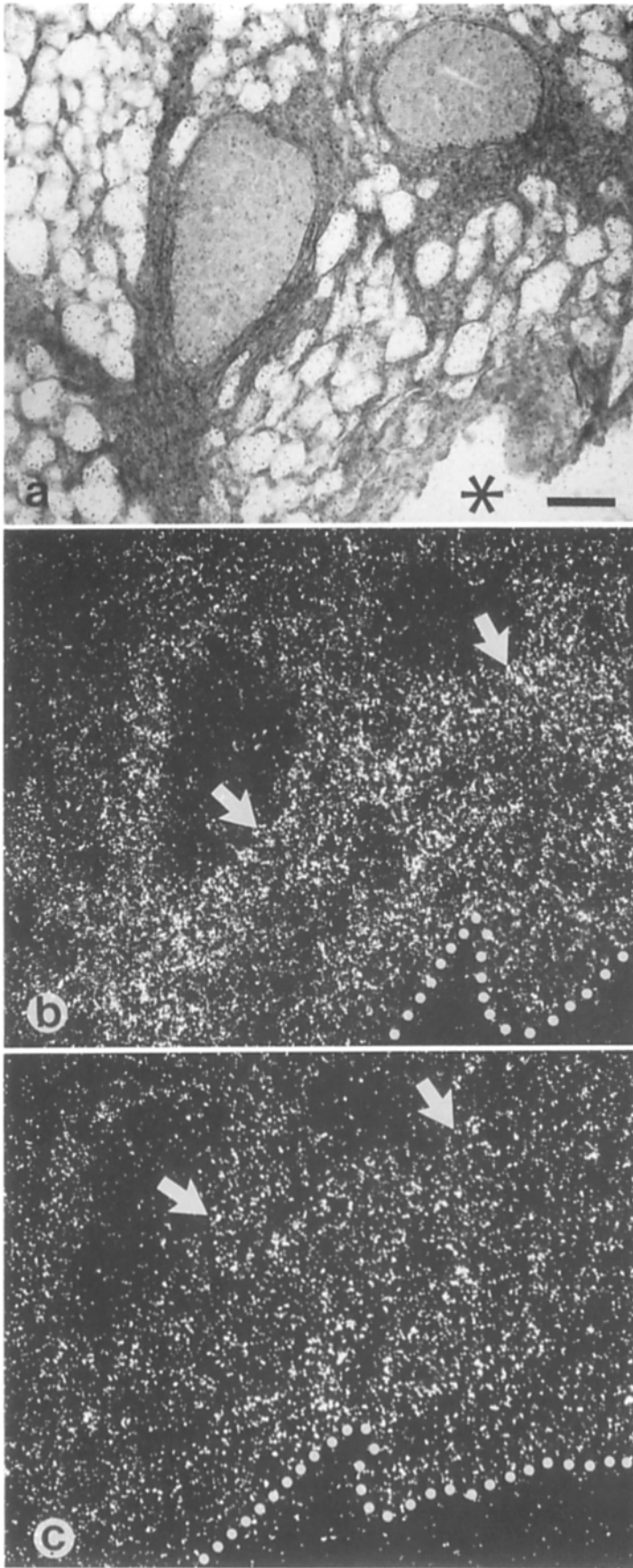
Figure 6. Photomicrographs of ^{35}S autoradiography showing the effect of chondroitinase ABC digestion of sections of mammary gland in the vicinity of a TGF-β1 implant (150 ng/24 h). (*a*) Alcian blue–stained section showing two end buds (the topmost seen in cross-section) adjacent to a TGF-β1 implant (*). (*b*) Section incubated for 4 h in digest buffer minus enzyme. Silver grains are concentrated in the matrix at the epithelial–stromal interface closest to the implant (*arrows*); the implant border is bounded by white dots. (*c*) Section adjacent to that pictured in *b*, digested for 4 h had ∼50% fewer silver grains between the epithelial–stromal boundary of the end bud (*arrows*) and the implant. Similar results were obtained by digesting with testicular hyaluronidase. Bar, 50 μm.
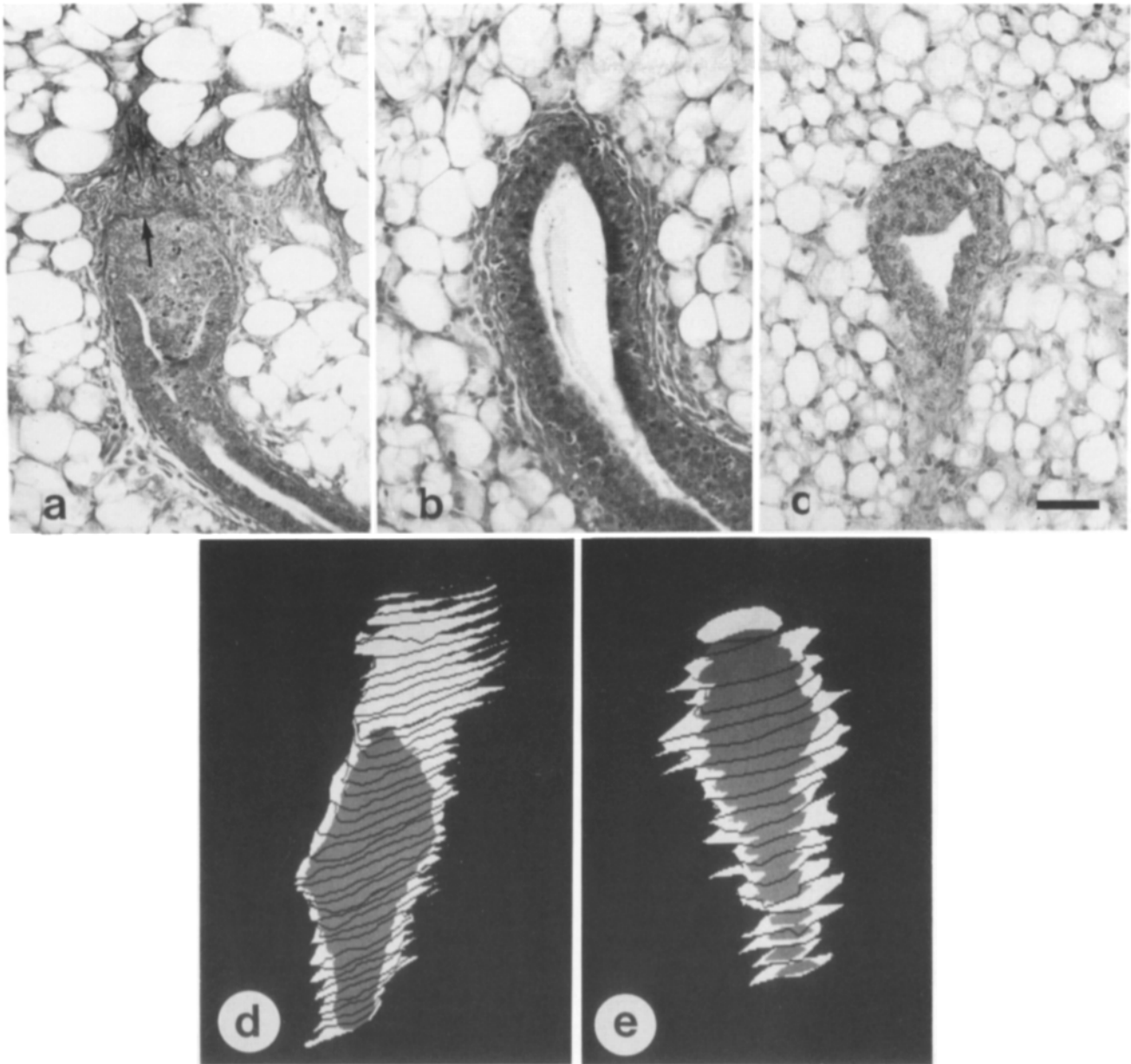
Figure 7. Comparison of pattern of extracellular matrix deposition around TGF-β1- and EGF-affected end buds with normally involuted duct tips. (*a*) End bud treated for 24 h with 150 ng TGF-β1. Arrow points to the epithelial–mesenchymal interface. (*b*) Tip of normally involuting duct. Note the approximately even thickness of the fibrous investment on the duct sides and around the tip. (*c*) End bud treated with EGF (21 μg/72 h). At 3 d, EGF treatment resulted in an 85% reduction in DNA synthesis as determined by thymidine autoradiography with end bud involution following at later time-points (5). Bar in *a*, *b*, and *c*, 50 μm). (*d* and *e*) Three-dimensional computer reconstructions of treated and control end buds emphasize the matrix induced by TGF-β1. End buds are different than those pictured in *a* and *b*. Fibrous stroma is represented by the unshaded zones surrounding the (gray) end buds.

the participation of adjacent epithelium. Two hypotheses are suggested. First, the action of exogenous TGF-β1 may be directly on the mammary epithelium, inhibiting cell proliferation as previously reported (21), but not stimulating increased matrix synthesis per se. Here, the growth-inhibited epithelium organizes the surrounding stromal cells, which are already engaged in ECM synthesis, to form a periductal investment when the epithelium fails to continue its outgrowth.

This suggestion explains the absence of organized ECM synthesis around the TGF-β1 implant, and is supported by

the observation that scattered stromal cells exhibit a considerable degree of background ECM synthesis (Figs. 2, *b* and *d*, and 6 *b*). The notion of mammary epithelium as an organizational center is also supported by histological studies on which the three-dimensional reconstructions were based (Fig. 7), in which it frequently appeared that stromal cells were aligned in "streams," perhaps responding to chemotactic signals from the inhibited epithelium. A purely inhibitory role for exogenous TGF-β1 is not consistent, however, with the observation that intense, ectopic ECM synthesis was present only in TGF-β1-treated gland, and was not observed

in untreated growth-restricted gland, or in gland inhibited by treatment with exogenous EGF or dexamethasone (Fig. 7).

A second hypothesis is that, in addition to exogenous TGF-β1, an unknown diffusible factor of epithelial origin is required to stimulate periductal extracellular matrix synthesis and deposition. A diffusible factor is considered more likely than signaling through cell–cell contacts, because the basal lamina around the end bud and duct is continuous, and contacts between epithelial and stromal cells have not been observed (24).

A putative epithelial factor might operate by sensitizing nearby mesenchymal cells to respond to TGF-β1, which then stimulates ECM synthesis. The unusual amounts of TGF-β1 released by the implant could result in the observed ectopic ECM synthesis. Alternatively, the epithelium could release a factor in response to TGF-β1 that directly stimulated stromal synthesis of matrix components. Either model would account for the epithelial requirement of TGF-β1 action and would explain the absence of matrix stimulation around the implant.

The epithelium requirement for mammary ECM synthesis in response to TGF-β1 contrasts with several in vitro studies which, with limited exceptions (8, 9), show TGF-β1 to be capable of stimulating the synthesis of extracellular matrix components unassisted (15). While some of these results may reflect the adaptation of cells to long-term culture, TGF-β1 also enhanced the synthesis of glycosaminoglycan in primary cultures treated soon after isolation (4, 25). These results indicate tissue- and cell-specific requirements for stimulation of matrix synthesis.

The condensation of fibrocytes and the synthesis of matrix around mammary epithelium is similar in certain respects to epithelial-mesenchymal interactions in the developing male urogenital tract that lead to the programmed involution of the female urogenital anlagen (23). In this case, testicular Sertoli cells synthesize Mullerian inhibiting substance (MIS), which induces the aggregation of mesenchymal cells and the deposition of a chondroitin sulfate-rich extracellular matrix around the female epithelial anlagen. Ductal resorption follows. As with the mammary results reported here, the MIS effect is exquisitely localized, and the mesenchymal response is clearly organized by the epithelium.

These similarities between the mammary gland and Mullerian duct suggest that TGF-β1, or molecules with similar activities, may normally act in conjunction with tissue-specific agents in a variety of developing tissues to mediate epithelial-mesenchymal interactions. This notion is supported by the immunohistochemical localization of TGF-β1 in numerous mouse embryonic tissues at sites where epithelium-mesenchyme interactions are occurring (10).

Our results, showing specific action of TGF-β1 on epithelium-dependent ECM synthesis in vivo, may be helpful in interpreting recent data showing the presence of endogenous TGF-β1 in mammary ducts and their surrounding stroma (Daniel et al., unpublished). In our present study, the ectopic location of ECM synthesis was unusual, due presumably to the mode of growth factor delivery in which abnormal concentrations of the growth factor were delivered at the end bud tip. Nevertheless, the demonstrated ability of TGF-β1 to stimulate ECM in a specific, epithelium-dependent manner, suggests a role for endogenous TGF-β1 in the organization of periductal stroma, perhaps by mediating an epithelium-stroma interaction.

References

1. Arteaga, C. L., A. K. Tandon, D. D. Von Hoff, and C. K. Osborne. 1988. Transforming growth factor beta: potential autocrine growth inhibitor of estrogen receptor-negative human breast cancer cells. Cancer Res. 48:3898–3904.
2. Bernfield, M. R., R. G. Cohn, and S. D. Banerjee. 1973. Glycosaminoglycans and epithelial organ formation. Am. Zool. 13:1067–1083.
3. Bissell, M. J., and H. G. Hall. 1987. Form and function in the mammary gland: the role of extracellular matrix. In The Mammary Gland: Development, Regulation, and Function. M. C. Neville and C. W. Daniel, editors. Plenum Publishing Corp., New York. 97–146.
4. Centrella, M., T. L. McCarthy, and E. Canalis. 1987. Transforming growth factor beta is a bifunctional regulator of replication and collagen synthesis in osteoblast-enriched cell cultures from fetal bone. J. Biol. Chem. 262:2869–2874.
5. Coleman, S., and C. W. Daniel. 1990. Inhibition of mouse mammary ductal morphogenesis and down-regulation of the EGF receptor by epidermal growth factor. Dev. Biol. 137:425–433.
6. Cox, K. H., D. V. DeLeon, L. M. Angerer, and R. C. Angerer. 1984. Detection of mRNAs in sea urchin embryos by in situ hybridization using asymmetric RNA probes. Dev. Biol. 101:485–502.
7. Daniel, C. W. 1989. TGF-beta-1-induced inhibition of mouse mammary ductal growth: developmental specificity and characterization. Dev. Biol. 134:20–30.
8. Falanga, V., S. L. Tiegs, S. P. Alstadt, A. B. Roberts, and M. B. Sporn. 1987. Transforming growth factor beta: selective increase in glycosaminoglycan synthesis by cultures of fibroblasts from patients with progressive systemic sclerosis. J. Invest. Dermatol. 89:100–104.
9. Fine, A., and R. H. Goldstein. 1987. The effect of transforming growth factor-beta on cell proliferation and collagen formation by lung fibroblasts. J. Biol. Chem. 262:3897–3902.
10. Heine, U. I., E. F. Munoz, K. C. Flanders, L. R. Ellingsworth, P. H. Lam, N. L. Thompson, A. B. Roberts, and M. B. Sporn. 1987. Role of transforming growth factor beta in the development of the mouse embryo. J. Cell Biol. 105:2861–2876.
11. Kimelman, D., and M. Kirschner. 1987. Synergistic induction of mesoderm by FGF and TGF-beta and the identification of an mRNA coding for FGF in the early Xenopus embryo. Cell. 51:869–877.
12. Lopez-De Leon, A., and M. Rojkind. 1985. A simple micromethod for collagen and total protein determination in formalin-fixed paraffin-embedded sections. J. Histochem. Cytochem. 33:737–743.
13. Penttinen, R. P., S. Kobayashi, and P. Bornstein. 1988. Transforming growth factor beta increases mRNA for matrix proteins both in the presence and in the absence of changes in mRNA stability. Proc. Natl. Acad. Sci. USA. 85:1105–1108.
14. Rasmussen, S., and A. Rapraeger. 1988. Altered structure of the hybrid cell surface proteoglycan of mammary epithelial cells in response to transforming growth factor beta. J. Cell Biol. 107:1959–1967.
15. Rizzino, A. 1988. Transforming growth factor beta: multiple effects on cell differentiation and extracellular matrices. Dev. Biol. 130:411–422.
16. Roberts, A. B., K. C. Flanders, P. Kondaiah, N. L. Thompson, E. van Obberghen-Shilling, L. Wakefield, P. Rossi, B. de Crombrugghe, U. Heine, and M. B. Sporn. 1988. Transforming growth factor beta: biochemistry and role in embryogenesis, tissue repair and remodeling, and carcinogenesis. Rec. Prog. Hormone Res. 44:157–197.
17. Scharffetter, K., W. Stolz, B. Lankat-Buttgereit, C. Mauch, M. Kulozik, and Th. Krieg. 1989. In situ hybridization: a useful tool for studies on collagen gene expression in cell culture as well as in normal and altered tissue. Virchows Arch. B Cell Pathol. 56:299–306.
18. Silberstein, G. B., and C. W. Daniel. 1982. Elvax 40P implants: sustained, local release of bioactive molecules influencing mammary ductal development. Dev. Biol. 93:272–278.
19. Silberstein, G. B., and C. W. Daniel. 1982. Glycosaminoglycans in the basal lamina and extracellular matrix of the developing mouse mammary duct. Dev. Biol. 90:215–222.
20. Silberstein, G. B., and C. W. Daniel. 1984. Glycosaminoglycans in the basal lamina and the extracellular matrix of serially aged mouse mammary ducts. Mech. Age. Dev. 24:151–162.
21. Silberstein, G. B., and C. W. Daniel. 1987. Reversible inhibition of mammary gland growth by transforming growth factor-beta. Science (Wash. DC). 237:291–293.
22. Silberstein, G. B., P. Strickland, V. Trumpbour, S. Coleman, and C. W.

Daniel. 1984. In vivo, cAMP stimulates growth and morphogenesis of mouse mammary ducts. *Proc. Natl. Acad. Sci. USA.* 81:4950–4954.

23. Wartenberg, H. 1985. Morphological studies on the role of the periductal stroma on the regression of the human male Mullerian duct. *Anat. Embryol.* 171:311–323.

24. Williams, J. M., and C. W. Daniel. 1983. Mammary ductal elongation: Differentiation of myoepithelium during branching morphogenesis. *Dev. Biol.* 97:274–290.

25. Wrana, J. L., M. Maeno, B. Hawrylyshyn, K.-L. Yao, C. Domenicucci, and J. Sodek. 1988. Differential effects of transforming growth factor-beta on the synthesis of extracellular matrix proteins by normal fetal rat calvarial bone cell populations. *J. Cell Biol.* 106:915–924.